Geophys. J. Int. (1992) **113,** 252–259

RESEARCH NOTE

Preliminary observations from the use of US–Soviet Joint Seismic Program data to model upper mantle triplications beneath Asia

E. J. Garnero,[1] D. V. Helmberger[1] and L. J. Burdick[2]

[1]*Seismological Laboratory, 252–21, Caltech, Pasadena, CA* 91125, *USA*
[2]*Woodward-Clyde Consultants,* 566 *El Dorado, Pasadena, CA* 91101, *USA*

Accepted 1992 August 17. Received 1992 August 12; in original form 1991 December 27

SUMMARY

New short-period waveform data from the US–Soviet Joint Seismic Program (JSP) make possible investigations of Asian upper mantle structure. The goal of this paper is to explore the potential use of the newly available JSP data to gain a qualitative view of upper mantle structure beneath Asia, and to facilitate more detailed future detailed future upper mantle studies. In a reconnaissance approach, waveform upper mantle studies. In a reconnaissance approach, waveform predictions from upper mantle *P*-wave velocity models of previous studies are compared to the JSP data to investigate regional differences in the central Asian upper mantle. Data coverage brackets the upper mantle triplications with excellent multi-source-to-stations sections. The abundance of data for controlled source–receiver geometries and the impulsive nature of the arrivals enable us to stack seismograms to improve signal-to-noise ratio. Arrivals from the 400 and 670 km discontinuities are apparent in the data and are compared to predictions of the mantle models. The principal result is that, for the regions studied, paths through cratonic regions of Asia are compatible with shield-type models, while paths through highly deformed regions of Asia are compatible with models derived for tectonically active regions, suggesting large lateral variations beneath the Eurasian continent. Use of the JSP data in a comparative approach is fast and simple, and proves effective in obtaining a first-order understanding of the Asian upper mantle. This result also presents the potential for qualitative studies elsewhere with digital portable stations.

Key words: stacking, synthetic seismograms, triplications.

1 INTRODUCTION

Until recently, data recorded in central Asia have not been readily available, preventing the Asian plateau from being an area of prolific study. Through the US–Soviet Joint Seismic Program (JSP) between IRIS and the Soviet Academy of Sciences, seismograms recorded over many decades on the Soviet national short-period network are now available. This network is similar in many respects to the short-period World Wide Seismographic Station Network (WWSSN; Given, Helmberger & Zhao 1991). These data greatly increase the number of event-to-station paths in central Asia and span a distance range which brackets upper mantle triplications. The purpose of this note is to pursue the potential usefulness of this type of data for providing first-order information on the Earth's upper mantle, as well as facilitating future, more detailed studies.

We analyse *P*-wave motions at distances where arrivals from the upper mantle triplications are clearly evident. An approach is taken wherein data are compared to predictions made from upper mantle models presented in previous studies. These models were derived for distinctly different regions elsewhere on the globe, and are used here in an effort to gain a qualitative understanding of the lateral variations in the upper mantle of the different locales of central Asia.

2 THE DATA SET

The data set is a collection of 479 digitized short-period (SP) vertical component records from 11 stations of the Soviet

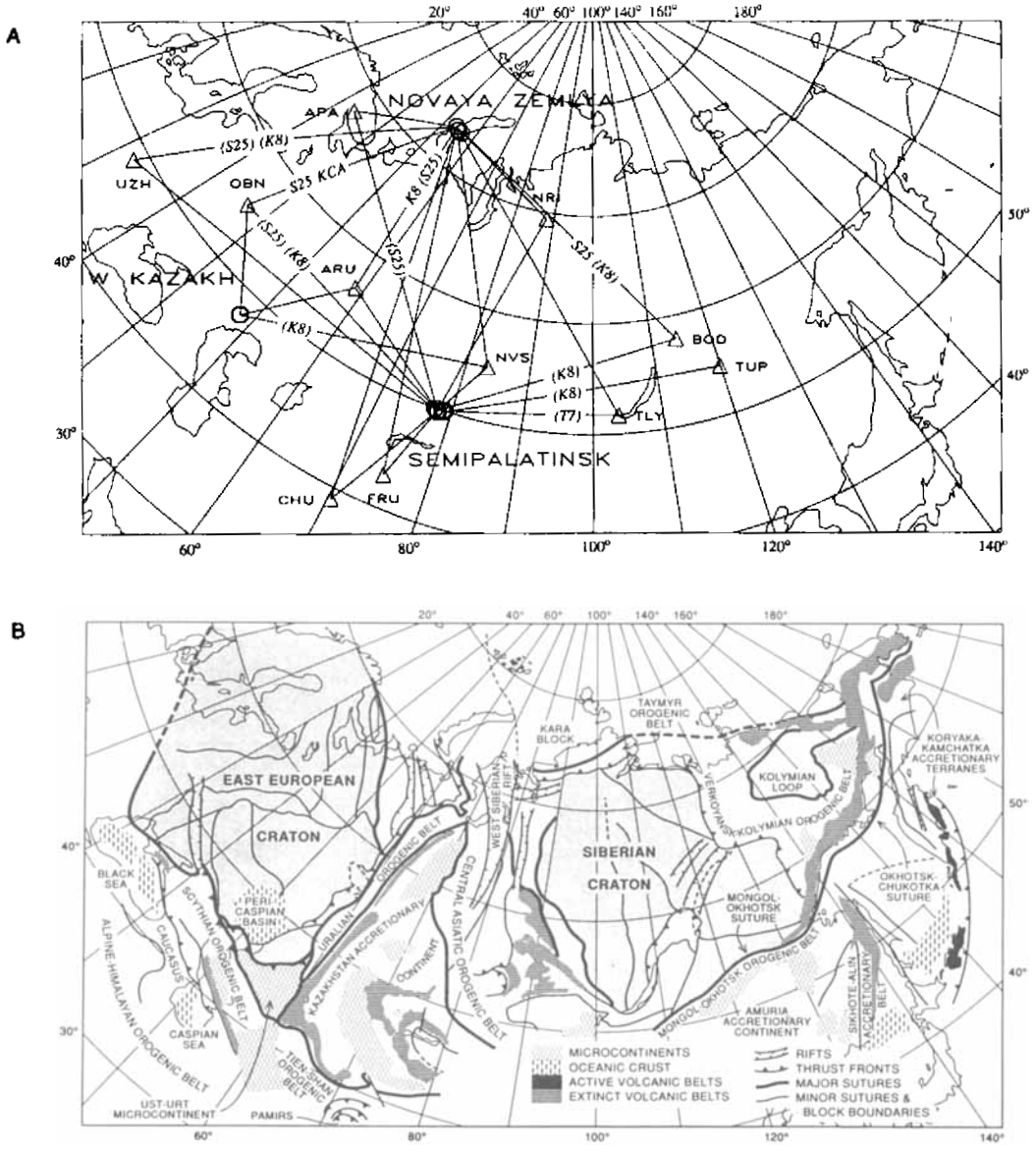

Figure 1. (a) Map indicating the locations of three source regions (circles) and 11 Soviet stations (triangles) used in this study. Names of best-fitting models are printed on ray paths. (b) Main structural elements of Asia (from Zonenshain *et al.* 1991). The scale and projection are the same for both (a) and (b).

national network, recording 110 underground nuclear explosions. A map of the study area showing sources, paths and receivers is presented in Fig. 1(a). This array spans distances from around 5° to 40°, sampling many different regions, as well as different tectonic settings (Fig. 1b). The number of events recorded at each station varies from less than 10 to over 100. Over half of the data are in the distance range 15° to 27°, where triplication arrivals are routinely observed. Nearly all of the 110 events are from the two main Soviet test sites, Semipalatinsk and Novaya Zemlya, with the exception of several off-site Peaceful Nuclear Explosions (PNEs.) United States Geological Survey (USGS) PDE locations were used in the calculation of all distances. The Semipalatinsk events are from three specific sites: Degelen Mountain, Koynstan and Shagan River, and the data from each site were analysed separately. The CKM-3 SP instruments recording these events peak at around 1 s.

Signals were stacked to improve the signal-to-noise ratio (SNR). Recordings of events from a single-source region at a single station were binned separately and a separate stack was made for each, provided sufficient data existed for any given path. Thus, for any given station, up to four stacks may have been made: one for each of the three Semipalatinsk sites, and one for the Novaya Zemlya site. The data for specific station–source region pairs contain similar waveforms, and distances for data in any stack usually vary by less than 30 km. Stacks were made by lining up the first arrivals of the waveforms. All amplitudes were normalized to unity before stacking. An example for station OBN is given in Fig. 2. The distance window, using the USGS PDE locations, spans only about 7 km. The arrivals after the triplication arrivals have been reduced in amplitude by the stacking procedure. Resulting stacked traces are used in the modelling procedure in the rest of this paper. Records

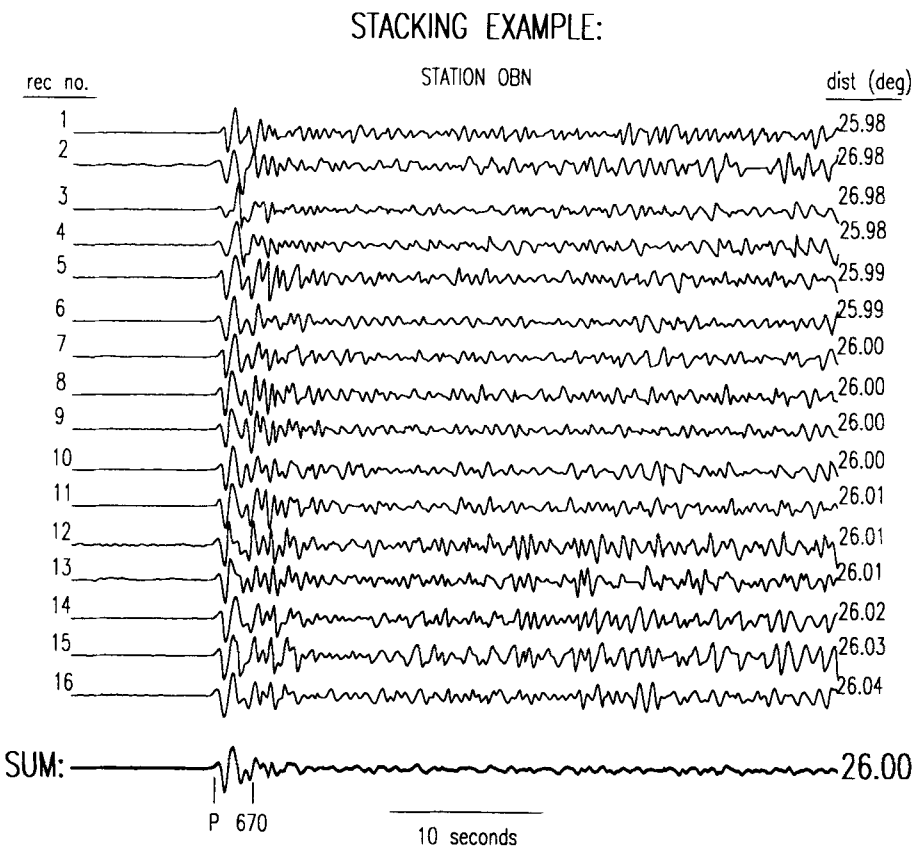

Figure 2. Example of a data stack for station OBN from Shagan River events. The timing predictions from model S25 of the direct, 400 km, and 670 km discontinuities are also indicated.

were stacked only for distances where triplication arrivals are clearly seen above the noise level. Of the 479 records in this data set, 183 were used to make 20 stacks, with the average number of records per stack being about 9 (Table 1).

3 COMPARATIVE MODELLING APPROACH

The approach used in this study is to compare data with predictions made from models previously presented in the literature. The synthetics were generated by the generalized ray method (Helmberger 1973). The procedure was first to generate Green's functions for the specific models and distances and then to convolve them with empirical source functions to obtain the predictions. Empirical source functions were estimated by selecting first arrival *P*-wave waveforms at distances where triplication arrivals do not interfere with the *P*-wave, then using the time window of the first arrival for convolution with synthetics. Only records with good signal-to-noise ratio as well as minimal *P*-wave coda were used in the procedure. This approach inherently includes the CKM-3 instrument response. For each data stack, a *P*-wave (source function) was selected that had a similar pulse width as the first pulse of the data stack, as an attempt to accomodate attenuation effects. Effects such as differential attenuation of the triplication phases and site reverberation are not included in the synthetics. Nevertheless, upper mantle triplication arrivals are above the noise level in the data and data stacks, and will be compared to model predictions.

Table 1. Stacked traces list.

STACK NO.	STA NAME	DELTA (deg)	# RECS	SOURCE REGION	SITE NAME
1	ARU	13.43	3	Semipalatinsk	Degelen Mountain
2	ARU	13.75	4	Semipalatinsk	Shagan River
3	TLY	15.72	14	Semipalatinsk	Shagan River
4	ARU	17.09	9	Novaya Zemlya	Matochkin Shar
5	OBN	19.76	7	Novaya Zemlya	Matochkin Shar
6	NRI	20.14	4	Semipalatinsk	Koynstan
7	NVS	21.86	8	Novaya Zemlya	Matochkin Shar
8	BOD	22.01	4	Semipalatinsk	Shagan River
9	BOD	22.49	3	Semipalatinsk	Degelen Mountain
10	NVS	22.87	4	W. Kazakh	PNE
11	APA	24.36	2	Semipalatinsk	Degelen Mountain
12	APA	24.60	2	Semipalatinsk	Shagan River
13	OBN	25.22	5	Semipalatinsk	Koynstan
14	TUP	25.28	5	Semipalatinsk	Shagan River
15	OBN	25.56	17	Semipalatinsk	Degelen Mountain
16	OBN	25.96	39	Semipalatinsk	Shagan River
17	BOD	27.44	9	Novaya Zemlya	Matochkin Shar
18	UZH	28.31	5	Novaya Zemlya	Matochkin Shar
19	TLY	29.88	5	Novaya Zemlya	Matochkin Shar
20	UZH	36.20	31	Semipalatinsk	Shagan River

Synthetic seismograms were generated for the distances in Table 1 for four different models. The models chosen represent different types of lithospheric structure (Fig. 3), such as: a thick shield model S25 (LeFevre & Helmberger 1989, Canadian shield); a model with no low-velocity zone KCA (King & Calcagnile 1976, western Russia); two models with a low-velocity zone in the lithosphere; K8 (Given & Helmberger 1980, northwestern Eurasia); and T7 (Burdick & Helmberger 1978, western US).

The four models chosen for this comparative study

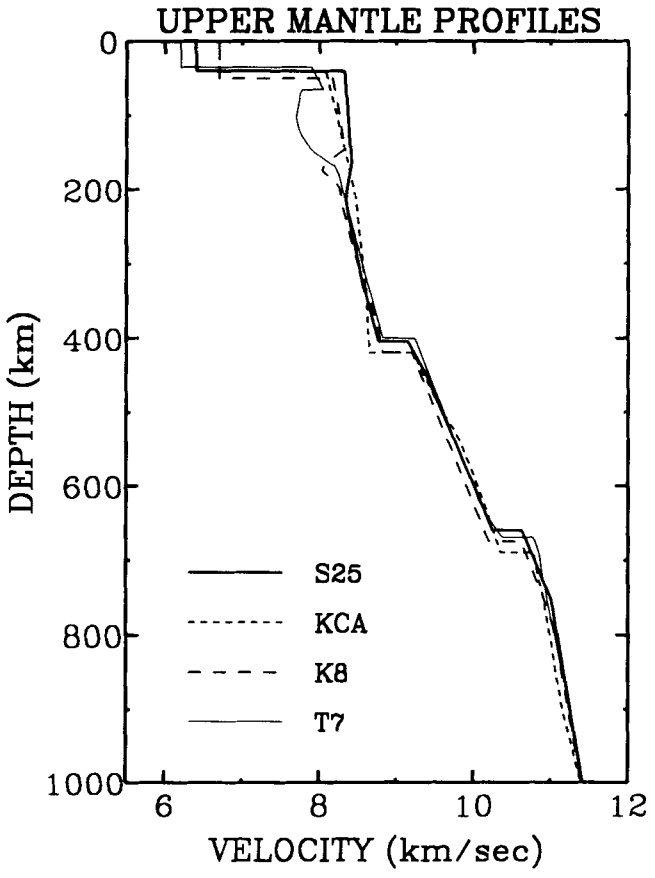

Figure 3. *P*-wave velocity models used in this study.

represent widely varying upper mantle structures, and were all derived from body wave studies. KCA is a logical choice as a comparison model because it was derived from short-period data in the western Russia region. K8 was chosen because it has a shield-like lithosphere as well as being derived for parts of central Asia that coincide with our study area. K8 was constructed using KCA as a starting model, utilizing both short- and long-period data from Soviet explosions. A classic shield model is S25, derived for the Canadian shield region using long-period earthquake data. A first-order justification in choosing S25, a model derived for a completely different locale, is that central Asia is thought to be shield-like, with the East European Craton to the west and the Siberian Craton to the east. This choice has proven useful, as S25 is a best-fitting model for several of the paths in our study area. To assess regions where tectonics are thought to play an important role, model T7 was utilized. Model T7 was derived for the tectonic western US from long-period body waves of earthquakes and explosions. Other models in the literature may have done equally well for our criteria of choosing models with fundamentally differing lithospheres. We note again that our choice of models is to emphasize regional and lateral variations in the upper mantle beneath Asia, and not to make an argument for specific models for the specific locales.

The most important differences in these models are in the top 200 km. Second-order differences are the depths of the 400 and 670 km discontinuities, gradients above and below the discontinuities, as well as the per cent velocity increase of the discontinuities. For the rest of this paper we loosely use the numbers '400' and '670' to represent the two major upper mantle discontinuities, keeping in mind that their exact depth varies from model to model, as well as most likely in the Earth.

4 ABSOLUTE TRAVELTIMES

The traveltimes from first arrivals were usually very easy to measure due to the first arrival's impulsive nature. Records having low signal-to-noise ratio were not used in our traveltime analysis. One of the uncertainties in the traveltimes arises from the use of the USGS PDE origin times (unfortunately, the Soviet origin times are not yet available). Also, all data came from the Center for Seismic Studies (CSS) with a file of instrument time corrections ranging from 0–60 s with as many as three time corrections per day for each station. In many cases, the clock error was not constant over the period of a day, and changed by as much as 1.5 s. This is another source of absolute traveltime error. For cases where the clock error changed within a day, we linearly interpolated the given time corrections for that day to the *P*-wave arrival time for that day's event. Obviously, timing remains a serious problem.

First arrival traveltimes are shown in Fig. 4 with the predictions of model KCA. Anomalies are clearly visible in the figure, especially at 15.7° (station TLY, indicated by the arrow) where times are delayed by around 8 s. This may be due to a slow tectonic path (see Fig. 1b). Uncertainties in absolute traveltimes are too large (owing to clock errors of greater than 1 s as well as origin time uncertainties) to be useful in this study. Also, $dT/d\Delta$ could not be used because source–receiver distances are not evenly distributed.

5 WAVEFORM COMPARISONS

As Fig. 1 indicates, our study area has good coverage of the central Asia area. However, without a profile of stations for

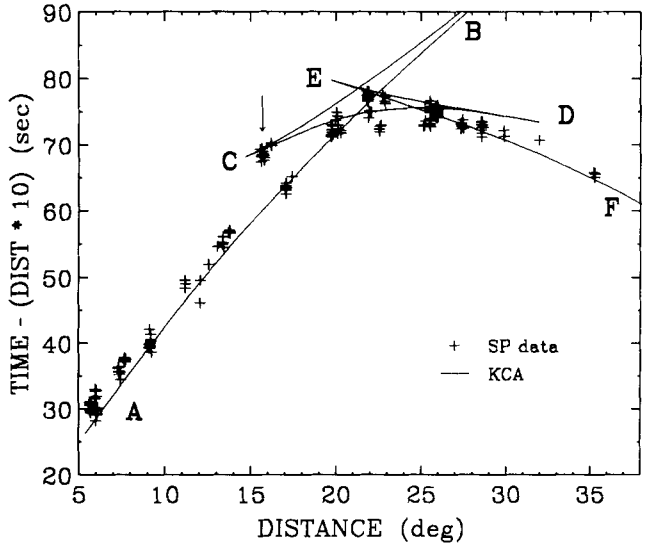

Figure 4. First arrival picks made from impulsive waveforms only are shown here with the prediction of model KCA. The letters A–F represent the names of the different triplication branches. The arrow indicates the late times of station TLY.

a specific path, it is not possible to obtain a unique solution model, although comparisons with model predictions can still be made to assess agreement with different classes of model and to investigate qualitatively lateral variations from path to path. Predictions for the models K8, KCA, S25 and T7 are compared to the data stacks in Fig. 5. Nine panels are presented, in each of which the top trace is the data stack, and the four underlying traces are model predictions. The time window shown is 30 s. Due to traveltime and amplitude uncertainties, the first arrivals have been lined up and maximum amplitudes normalized to unity. In comparing the data to predictions, the relative amplitudes and timing of the different triplication arrivals will be discussed. Up to around 21° the first arrival is the direct P from above the 400 (P_{AB}), and the second arrival is the combination of the reflection off the top of the 400 km discontinuity (P_{BC}) and the P-wave from below the 400 (P_{CD}). In some cases, the reflection off the top of the 670 (P_{DE}), along with the direct arrival from below the 670 (P_{EF}), is evident as a third arrival. This distance window corresponds to Figs 5(a) to (d). From right before the crossover distance of the P_{AB} and P_{CD}, to a little after the crossover of the P_{CD} and the arrival from below the 670 (P_{EF}), the differential time between the triplication arrivals is often too small to measure. This corresponds to

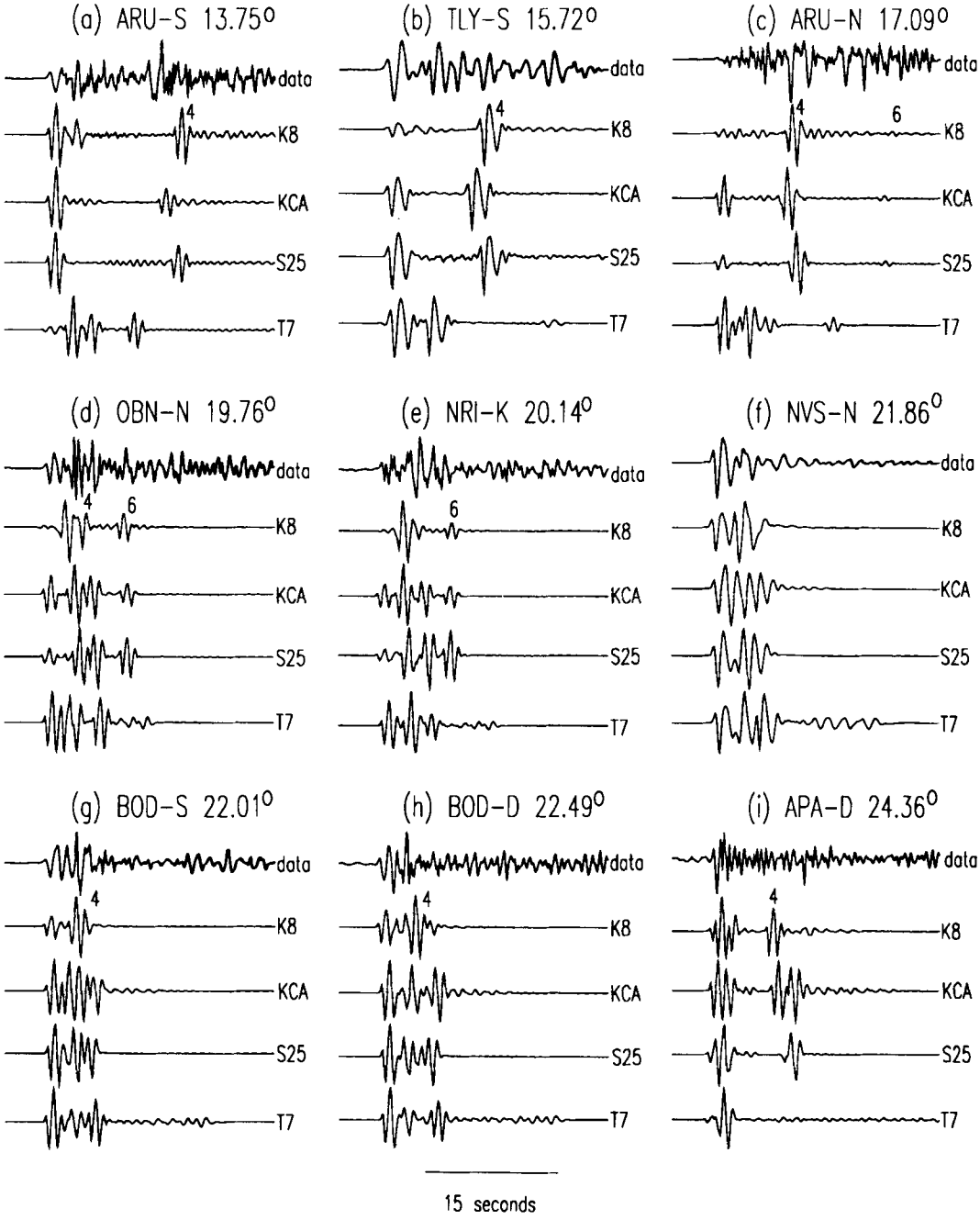

Figure 5. (a)–(i) present data stacks (top trace) and the predictions of the four models (bottom four traces.) The letter code next to the station names signifies the source location (D = Degelen Mountain, K = Koynstan, N = Novaya Zemlya, and S = Shagan River). Where the phases are well separated, the numbers '4' and '6' indicate arrivals from the 400 and 670 km discontinuities.

Figs 5(e) to (h), where at least two arrivals appear as more of a wave packet than distinct arrivals. The shapes of these wave packets (data and synthetics) are very sensitive to the amplitude ratios of the different arrivals. Beyond the crossover distance of P_{CD} and P_{EF} the arrivals separate in time, so that differential traveltime information again supplements the amplitude ratios.

Data from many of the paths to the west of the test sites in Fig. 1 are better modelled by a shield-type model. Data to TLY to the east from Semipalatinsk, however, are better modelled by the mixed-path western US model T7. Fig. 5(b) shows the data stack and predictions for station TLY. Only model T7 predicts the anomalously small differential traveltime between P_{AB} and P_{CD} due to its slow lid, which slows down the direct P with respect to the arrival from the 400 km discontinuity.

To a slightly more northerly azimuth is station BOD. There are two central Asian stacks for BOD, from the Shagan River and Degelen Mountain sites (Fig. 5g and h, respectively). For Fig. 5(g), the prediction from K8 is the best. An increase in distance by only 0.5° (Fig. 5h) yields a record that is poorly modelled by all four models. These complexities may be due to lateral variations along the path from a tectonic to a shield region as suggested by Fig. 1(b).

Station OBN recorded events from all three Semipalatinsk sites. The three resulting OBN data stacks and model predictions are presented in Fig. 6. For this distance, the first arrival is P_{EF} and the second arrival is a combination of P_{CD} and P_{DE}. Around 8 or 10 s after the first arrival, the back branch of the 400 triplication consisting of P_{AB} and P_{BC} can be seen in the synthetics. A remarkable feature in the data in Fig. 6 is the rapid decrease in amplitude with distance of the second arrival (P_{CD} and P_{DE}) with respect to the first arrival. This feature is not predicted in the synthetics. Given & Helmberger (1980) presented data in this same distance window from Semipalatinsk to an azimuth to the southwest recorded at TAB (Tabriz, Iran). For that azimuth, the changing amplitude ratio of the first two arrivals is well predicted by K8. The OBN data, however, appear anomalous in that the second arrival decays so rapidly in such a small distance window of around 0.8°. This feature of diminishing P_{CD} and P_{DE} relative to P_{EF} in a small distance window may be more accurately modelled by increasing the velocity gradient between the 400 and 670 discontinuities. An increase of the gradient causes downgoing rays in this depth range to turn up more sharply. Thus the deepest possible ray propagating above the 670 discontinuity, i.e., the arrival at the tip of the D branch, is bent up to a smaller distance.

Station TUP has an azimuth from Semipalatinsk intermediate to that of stations TLY and BOD for that same source region. For this path, the distance to TUP is 25.28°. This distance is in the window of that presented in Fig. 6 to station OBN, though the waveforms are quite different (Fig. 7a). The source time function of the TUP record is longer period, which may partly obscure any differentiation between the two triplication phases that are arriving just a few seconds apart. If these waves propagate through a transition zone from a tectonic lithosphere to that of a shield, complexities should be expected. The prediction from model K8 gives the closest fit. For paths to TLY, TUP and BOD from Semipalatinsk, the models K8 and T7 produce motions closest to our observations. This implies that, over a lateral distance of several 100 km or so, the low-velocity zone might drastically change from one like that in T7 to one like that in K8. The observations at larger

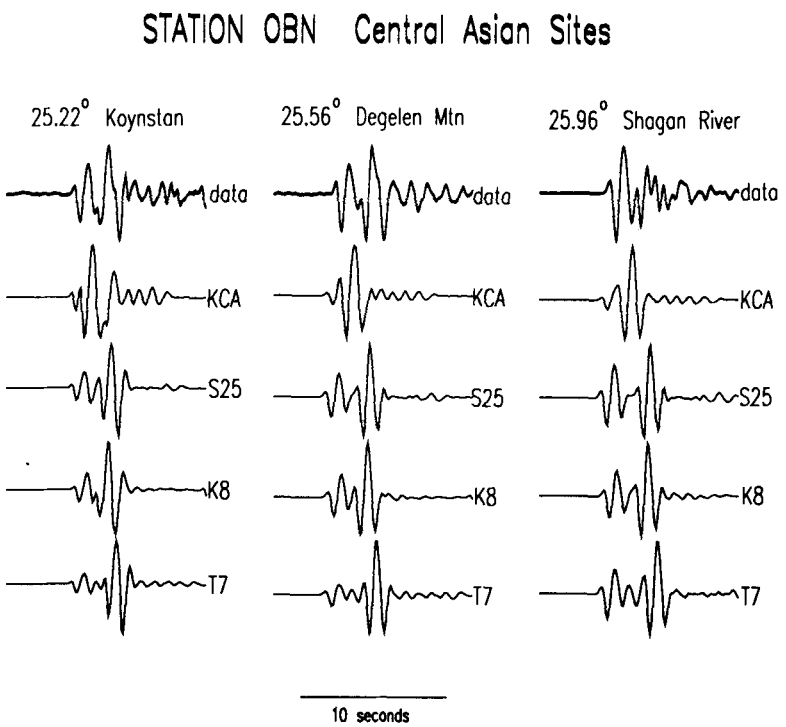

Figure 6. The three columns are separate stacks for events from the three Semipalatinsk sites recorded at station OBN (data are top trace, model predictions are bottom four traces). For these distances, the reflection off the 670 arrives around 2 or 3 s after the first arrival, and the 400 arrives outside the time window presented.

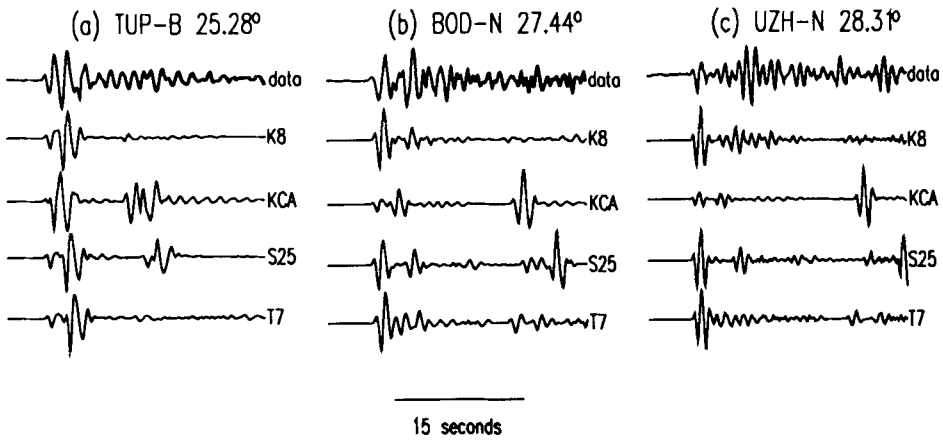

Figure 7. (a)–(c) present data stacks (top trace) and the predictions of the four models (bottom four traces).

distances (Figs 7b and c) are poorly modelled by these synthetic predictions. The large second arrival in the data in Fig. 7(b) roughly has the expected timing for the 670 km triplication arrival but is too large in amplitude relative to the direct *P*. The difference time between the direct *P* and the 670 arrival in Fig. 7(c) is larger in the data than the predictions.

Although absolute traveltime information was not used in our modelling procedure because of uncertainties in hypocentre information, we can still make qualitative traveltime comparisons between the different stations. For example, data recorded at TLY from Semipalatinsk are anomalously slow by up to 8 s when compared to KCA predictions (see arrow in Fig. 4). Absolute traveltimes for the direct *P*-waves at this range for various models show considerable differences. A very large difference exists between S25 (pure shield) and GCA [pure tectonic, Walck (1984)], and is roughly 13 s. The traveltime for GCA at 15.7° is over 10 s slower than that of KCA, which brackets the TLY times in Fig. 4. T7 predicts an arrival time nearly 3 s earlier than the TLY times, so that modifications to that of a more tectonic model make it possible to match these late times. This may imply a more tectonic upper mantle for the path to TLY from Semipalatinsk.

The names of the best-fitting models in Figs 5, 6 and 7 are printed on the source–receiver paths in Fig. 1(a). For some paths, two models are listed because both did equally well in modelling the data stacks. The model name is in parentheses if the best-fitting model for that path poorly predicts observed motions. All of the models used in this study have an LVZ, with the exception of KCA. Only one path favoured KCA (station OBN from Novaya Zemlya), with predictions from S25 being equally satisfactory. A first-order qualitative conclusion from this comparative approach is that, from the four models chosen for comparison in this study, the north and the west regions of our study area favour shield (S25) or shield-type (K8) models, while the area to the southeast is probably a transition zone from a shield-type mantle to a more tectonic upper mantle (T7).

Observations from several paths in this study are poorly modelled in timing and/or amplitude of the relative triplication arrivals by the above models (e.g. Figs 5a,h,i, 6 and 7a,b,c). For example, in the case of station OBN (Fig. 6), the diminishing second arrival at 25.96° can be attributed to an early ending of the 'D' tip of the 670 km triplication. To produce such a feature in the synthetics, changes must be made to the model in the transition zone. Model changes made far above the 400 km discontinuity tend not to diminish the amplitude of the second arrival enough to match the data (as suggested by predictions in Fig. 6). However, as suggested by Scott & Helmberger (1983), differential scatttering and/or topographic relief on the 670 km discontinuity can alter this amplitude ratio. One way to end the 670 km triplication at a smaller distance would be to include a small zone of an increased velocity gradient on the top side of the 670 discontinuity. This turns rays up more sharply, thus decreasing the distance where the D tip of the triplication occurs. An example of such a scenario is presented in Fig. 8. The left column of synthetics is from K8, whereas the middle column is from a model where K8 has been modified by a small zone of increased gradient right above the 670 discontinuity (K8.1). The prediction of K8.1 at 26.0° adequately suppresses the second arrival. It has been recently proposed that the depth of the 670 km discontinuity may vary by as much as 20 km (Shearer 1991). A 670 km discontinuity occurring at a more shallow depth would also result in the D tip of the triplication ending sooner. An example of the discontinuity raised by 17 km along with a slightly increased overlying gradient is presented in the third column of Fig. 8 (K8.2). K8.2 also predicts the correct amplitude behaviour at 26.0° for station OBN. Due to non-uniqueness, more data in the region are needed to resolve such issues. However, the differences in the 670 triplication data presented here suggest relatively deep lateral variations, in agreement with Shearer (1991).

Synthetics were made for a model where S25 was modified by adding roughly a 2 per cent velocity increase at 500 km depth (as in Jones, Mori & Helmberger 1992). A discontinuity of this nature is not supported by the short-period data stacks used in this study.

6 CONCLUSIONS

By analysing the new JSP data set consisting of digitized short-period Soviet seismograms, we have demonstrated the usefulness of such data to make first-order inferences on the upper mantle beneath central Asia, as well as its lateral variations. The method used here may be easily applied elsewhere with digital portable stations. Our waveform and

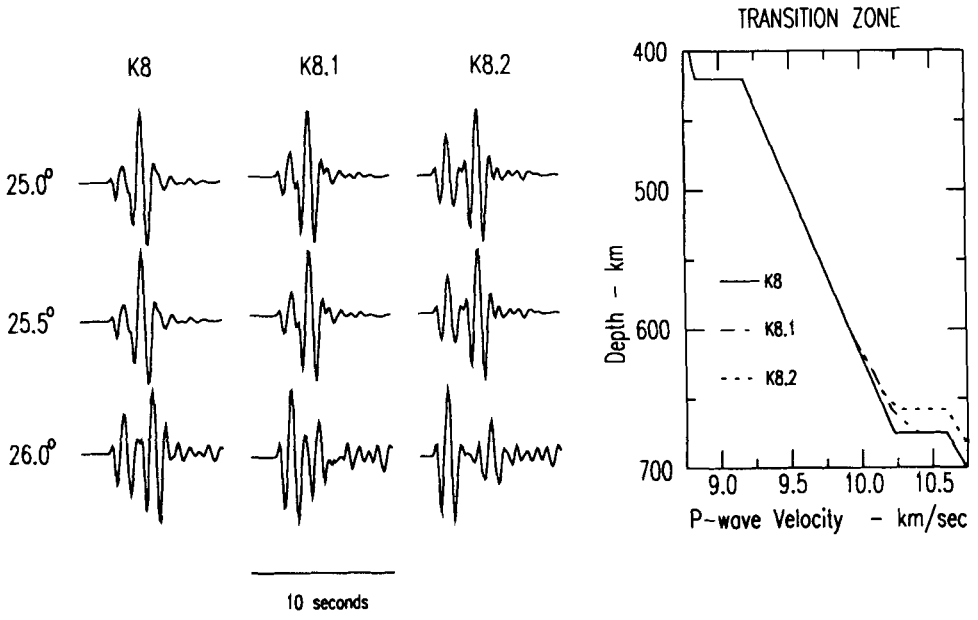

Figure 8. Predictions are presented for K8 and two models with increased velocity gradients right above the 670 km discontinuity (K8.1 and K8.2), where one has a more shallow 670 discontinuity by 17 km (K8.2).

differential traveltime comparisons indicate that large lateral variations are necessary to explain the observations from locale to locale. Most of our study area appears to be compatible with shield or shield-type models, while observations from regions to the south appear to be better modelled by tectonic models.

With broad-band data from the Soviet Union becoming more available, future work for this region will include a more detailed forward modelling effort. By using other stations in the Soviet national network that were not included in this data set, along with selected earthquakes, a better view of the Asian upper mantle may be constructed.

ACKNOWLEDGMENTS

The authors thank George Choy, Joan Gomberg and Peter Shearer for very constructive reviews, and Don L. Anderson, Laura Jones, and Paul Somerville for reading the manuscript. We also thank Paul Kovacs, Alan Ryall, and Richard Stead at CSS for assistance with the data set.

REFERENCES

Burdick, L. J. & Helmberger, D. V., 1978. The upper mantle *P* velocity structure of the western United States, *J. geophys. Res.*, **83,** 1699–1712.

Given, J. W. & Helmberger, D. V., 1980. Upper mantle structure of northwestern Eurasia, *J. geophys. Res.*, **85,** 7183–7194.

Given, H. K., Helmberger, D. V. & Zhao, L. S., 1991. A new aquisition of historical seismograms from the USSR emphasizing digital storage (abstract), *EOS, Trans. Am. geophys. Un.*, **72,** 190.

Helmberger, D. V., 1973. Numerical seismograms of long-period body waves from seventeen to forty degrees, *Bull. seism. Soc. Am.*, **63,** 633–646.

Jones, L., Mori, J. & Helmberger, D. V., 1992. Short period constraints on the proposed transition zone discontinuity, *J. geophys. Res.*, **97,** 8765–8774.

King, D. W. & Calcagnile, G., 1976. *P* wave velocities in the upper mantle beneath Fennoscandia and western Russia, *Geophys. J. R. astr. Soc.*, **46,** 407–432.

LeFevre, L. V. & Helmberger, D. V., 1989. Upper mantle *P* velocity structure of the Canadian shield, *J. geophys. Res.*, **94,** 17 749–17 765.

Scott, P. & Helmberger, D. V., 1983. Applications of the Kirckhoff–Helmholtz integral to problems in seismology, *Bull. seism. Soc. Am.*, **72,** 237–254.

Shearer, P., 1991. Constraints on upper mantle discontinuities from observations of long period reflected and converted phases, *J. geophys. Res.*, **96,** 18 147–18 182.

Walck, M. C., 1984. The *P*-wave upper mantle structure beneath an active spreading centre: the Gulf of California, *Geophys. J. R. astr. Soc.*, **76,** 697–723.

Zonenshain, L. P., Verhoef, J., Macnab, R. & Meyers, H. A., 1991. Magnetic imprints of continental accretion in the U.S.S.R., *EOS, Trans.*, **79,** 305–310.